IOPscience iopscience.iop.org

Home Search Collections Journals About Contact us My IOPscience

The electron density decay length effect on surface reactivity

This article has been downloaded from IOPscience. Please scroll down to see the full text article.

2010 J. Phys.: Condens. Matter 22 015001

(http://iopscience.iop.org/0953-8984/22/1/015001)

View the table of contents for this issue, or go to the journal homepage for more

Download details:
IP Address: 129.252.86.83
The article was downloaded on 30/05/2010 at 06:26

Please note that terms and conditions apply.

J. Phys.: Condens. Matter **22** (2010) 015001 (6pp) doi:10.1088/0953-8984/22/1/015001

The electron density decay length effect on surface reactivity

L Aballe[1], A Barinov[2], N Stojić[3,4,6], N Binggeli[5], T O Mentes[2], A Locatelli[2] and M Kiskinova[2]

[1] ALBA Synchrotron Light Facility, Carretera BP 1413, km 3.3, 08290 Cerdanyola del Vallés, Barcelona, Spain
[2] Sincrotrone Trieste S.C.p.A., Basovizza-Trieste 34012, Italy
[3] Scuola Internazionale Superiore di Studi Avanzati (SISSA), Via Beirut 2-4, Trieste 34014, Italy
[4] Theory @ Elettra Group, INFM-CNR Democritos, Trieste 34014, Italy
[5] Abdus Salam International Centre for Theoretical Physics and INFM-CNR Democritos National Simulation Center, Strada Costiera 11, Trieste 34014, Italy

Received 14 September 2009, in final form 30 October 2009
Published 2 December 2009
Online at stacks.iop.org/JPhysCM/22/015001

Abstract
The correlation between the thickness-dependent oxidation rate of ultrathin Al films on W(110) and the quantum-well states (QWS) resulting from electron confinement in the Al film has been explored by combined x-ray photoemission electron microscopy (XPEEM), low energy electron microscopy (LEEM), and first-principles calculations. Hybridization with substrate electronic states is observed to alter the film electronic structure, strongly modifying the electron density decay length in vacuum. The decay length, rather than the density of states at the Fermi energy, is found to dominate the observed reactivity trends.

(Some figures in this article are in colour only in the electronic version)

The quantitative understanding of surface reactivity in materials with reduced dimensionality remains a challenge for key technologies such as anti-corrosion coatings, catalysis, gas sensing, etc. The role of the local valence electron density in mediating the interactions with foreign species has long been recognized [1–4]. The electronic states and thus the reactivity are affected by the surface structure, the interfacial interactions [5, 6], the presence of defects or foreign atoms [7–11], and by quantum electron confinement, as demonstrated in recent studies of supported thin films [12–15]. In the latter case, oscillations in the oxidation rate of ultrathin Mg and Pb films with thickness were assigned to variations in an effective barrier dominated by the density of states (DOS) near the Fermi level (E_F) [12, 14, 15]. Theoretical studies, however, point to an explanation in terms of non-adiabatic effects [16] and a dominating role of the electron density decay length into vacuum λ [17, 18]. In the model system O_2/Al(111), a competition between the timescale corresponding to molecule–surface interaction and the time that the molecules spend near the surface has been suggested [19–22] to explain the striking differences between theory [23–25] and experiment [26, 27]. Nonetheless, the existence of an adiabatic energy barrier that is not reproduced by calculations could not be completely ruled out [28].

The previously studied Mg/W(110) system [12, 17, 18] behaves like free-standing films [29], in the sense that the DOS around E_F and λ oscillate in-phase as a function of thickness. In order to identify which of the two contributions dominates the thin-film reactivity, in the present work we replace Mg with Al. Al thin films have stronger electronic interactions with the substrate, to which, as we will show in this paper, λ is more sensitive than the DOS, making it possible to discriminate between the two effects.

The experiments were carried out using LEEM and XPEEM methods providing structural and chemical sensitivity, as described previously [12]. The morphology of Al layers grown on a clean W(110) substrate was monitored by LEEM and microspot low energy electron diffraction. The growth rate (0.2 ML min^{-1}) and substrate temperature (350–470 K) were optimized to obtain atomically flat regions, large enough for x-ray photoelectron microspectroscopy. This allows energy-filtered core level imaging on areas of different thicknesses under identical oxidation conditions, and thus a direct

[6] Present address: Abdus Salam International Centre for Theoretical Physics, Trieste 34014, Italy.

 © 2010 IOP Publishing Ltd Printed in the UK

comparison of the oxidation state with the film morphology. Under these conditions, the first two Al monolayers (ML) grow pseudomorphically on W(110), forming a compact bilayer, stable up to at least 850 K. The third ML grows on top with a slightly expanded hexagonal lattice (∼2.5% in one direction) in two domains, rotated by about ±3° around the [001] direction of W(110). The following growth proceeds layer-by-layer, with a relaxed Al lattice, and ±5° rotated domains [30].

The calculations were performed within density functional theory (DFT) using pseudopotentials and a plane-wave basis set, as implemented in the PWscf code [31]. We employed Troullier–Martins pseudopotentials using the Perdew–Burke–Ernzerhof exchange–correlation functional [32]. A kinetic energy cutoff of 49 Ryd was applied for the plane-wave expansion of the electronic orbitals of the Al/W system. The Al films were modelled using slab geometries in supercells.

We considered pseudomorphic and relaxed Al(111) films on W(110), in addition to free-standing Al slabs. Including the substrate and epitaxial distortions is important to fully understand the film electronic structure, because the lattice mismatch at the interface provides extra interaction channels for the partially confined electrons. The supported films were constructed of 7 ML of W(110), 2–7 ML of Al on one side, and 2 ML of Al on the other side, to avoid the presence of an electric field [18]. The vacuum region had a minimal thickness of 23 Å. For the free-standing film, we considered film thicknesses up to 12 ML, using the theoretical equilibrium Al bulk lattice parameter $a = 4.04$ Å, which coincides with the experimental value.

For the pseudomorphic film, a slab with the experimental tungsten lattice constant $a = 3.16$ Å was used, in order to keep the Al/W lattice mismatch, and hence the Al coherent strain, at its experimental values. The strain in the Al pseudomorphic film was $\varepsilon_{xx} = -0.10$ and $\varepsilon_{yy} = 0.10$, ($x \parallel$ W[1$\bar{1}$0] and $y \parallel$ W[001]). The atoms of the interfacial Al layer were located in the continuation of the W lattice. The relaxed film was modelled using an Al p(1 × 4) unit cell ('1 × 4-model'), and consisted of an unstrained Al film on top of a pseudomorphic Al bilayer on W(110). While the Al film had the unstrained lattice parameter $a = 4.04$ Å, the W lattice was strained ($\varepsilon_{xx} = -0.07$, $\varepsilon_{yy} = +0.07$, $\varepsilon_{xy} = +0.06$) to fit to the (1 × 4) cell of the Al unstrained lattice. The Al p(1 × 4) is a computationally-affordable-size unit cell to approach the incommensurate Al/W interface, which would require an infinite supercell. The surface unit cell for the '1 × 4-model' is given in figure 1. For k-points, we used a grid of (20, 5, 1) for the self-consistent calculations and of (48, 12, 1) for λ.

In the local DOS (LDOS) calculations, $\bar{\Gamma}$ states were used to simulate the normal photoemission spectra of the free-standing and pseudomorphic films, as done in previous work [33, 17]. In the case of the '1 × 4-model', however, due to the enlarged (1 × 4) surface unit cell (and resulting folding of the (1 × 1) surface Brillouin zone), Al states other than the relevant $\bar{\Gamma}$ states of the Al (1 × 1) film also appear in the supercell $\bar{\Gamma}$-state spectrum. In the LDOS calculations, these unwanted states of the '1 × 4-model' were filtered out by symmetrization in order to simulate the normal emission spectra of the films.

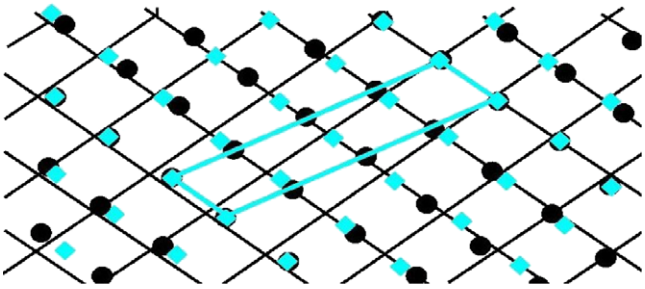

Figure 1. The surface unit cell shown by the light blue (grey in the printed version) solid line as used in the '1 × 4-model' calculations. The black circles represent Al atoms of the surface layer and the light blue (grey) diamonds represent the projection of W atoms of a corresponding layer in the substrate. For comparison, we also show the corresponding experimental W lattice (the underlying black grid of lines).

Valence band spectra of single-thickness Al micro-regions measured in normal emission are shown in figure 2(a). Homogeneous regions at the LEEM resolution level (10 nm) were selected for microspot spectroscopy. For the thinnest films the emission from the W substrate is still visible, although very soon dominated by a peak around ∼3 eV E_{binding} related to the Al bilayer, which with higher thickness evolves towards the bulk Al surface state at $E_{\text{binding}} = 4.6$ eV. The second peak, near 6 eV for 2 ML, can be assigned to the interface state, by comparison with the calculated density of states (see below). The characteristic bilayer emission can be distinguished up to about 5 ML, possibly in part due to small (<10 nm) uncovered areas of the bilayer. A distinct change in the line shape can be seen at 4 ML, induced by the entrance of a QWS. With increasing thickness more QWSs become occupied, crossing E_{F} at 6, 9, and 12 ML, with the three ML periodicity predicted by a simple particle-in-a-box model and the Al band structure [34]. The calculated LDOS for the pseudomorphic Al bilayer and for the 3–7 ML '1 × 4 model' films are compared to the measured spectra. The agreement is good for the thinner layers, and the Al-Shockley surface (SS) and interface states (IS), which shift closer to each other with thickness, can be identified in the spectra. However, above 4 ML there is a systematic difference: the calculations predict QWS crossing E_{F} for 7 and 10 ML instead of 6 and 9 ML, i.e. there is a rigid shift of +1 ML between theory and experiment. This shift is believed to be due to small differences between the DFT and experimental *bulk* band structures of Al: e.g. a ∼5% difference in the effective mass $m^*_{\Gamma-L}$ of the Al 3sp band below E_{F} could account for such a shift. This dependence on m^* is expected from the scaling of the energies, E_n, of the quantum-well levels, measured relative to the bottom of the Al 3sp band, as $E_n \sim 1/(m^* L^2)$, where L is the quantum-well width. Calculated *ab initio* effective masses are, indeed, often found to be more than 5% different from the experimental values [35]. We note that in the case of Mg/W(110) a larger shift of 2 ML was found, which was attributed in part to the presence of a large compressive lateral strain on the film near the interface (see [18]). In the case of Al/W(110), however,

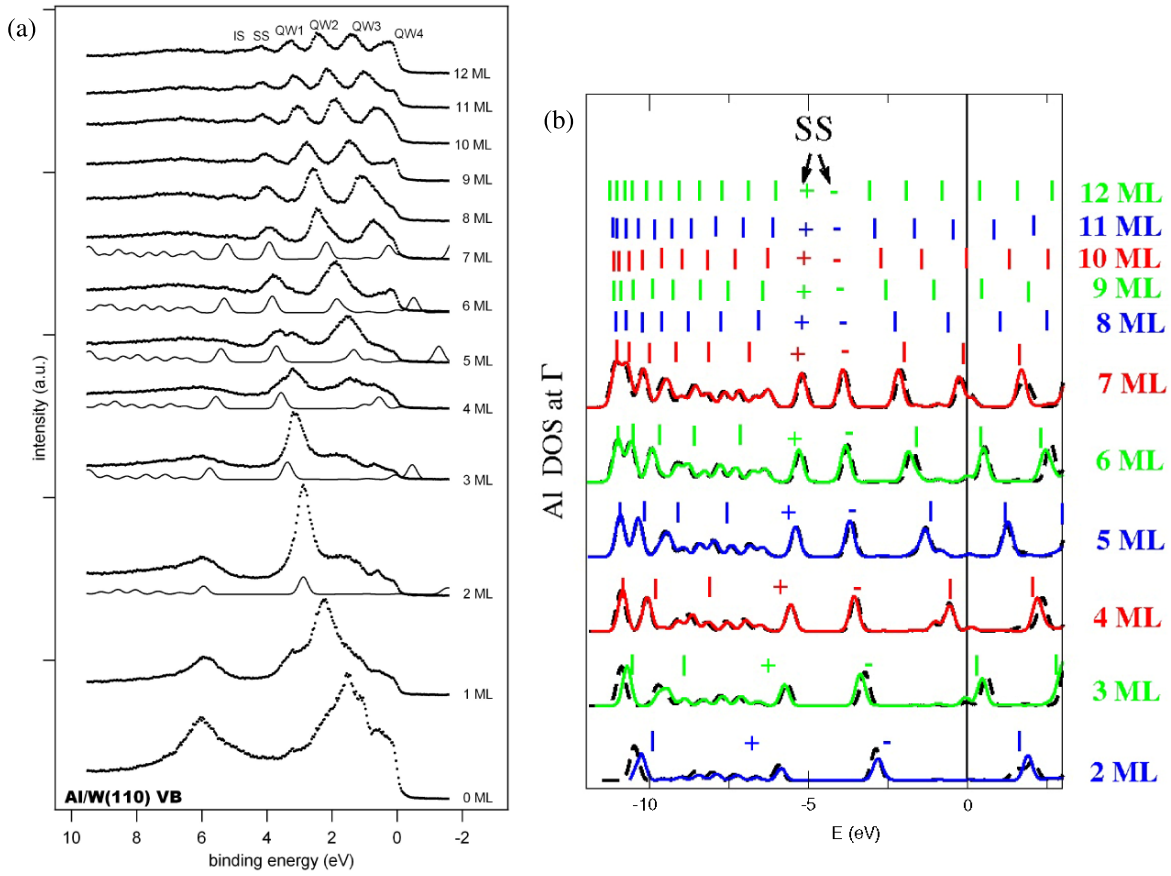

Figure 2. (a) Electronic structure of ultrathin Al films: valence band normal emission photoelectron spectra (dotted lines) from micro-areas of the indicated thickness ($E_{\text{phot}} = 60$ eV). Solid lines show the calculated LDOS spectra of the Al films at $\bar{\Gamma}$ for the pseudomorphic configuration at 2 ML and '1 × 4-model' configuration (see the text) at 3–7 ML. (b) Density of states at $\bar{\Gamma}$ calculated in the pseudomorphic configuration (black dashed lines), '1 × 4-model' configuration (colour solid lines), and energy levels at $\bar{\Gamma}$ of free-standing Al films (lines) for films of thickness of 2–12 ML. The states indicated by SS are derived from the Shockley surface states of the Al(111) free-standing film, which split into bonding (denoted by '+') and antibonding (denoted by '−') states across the Al slab. In the supported case, the latter (former) become predominantly surface (interface) states [18]. The zero of energy corresponds to the Fermi level.

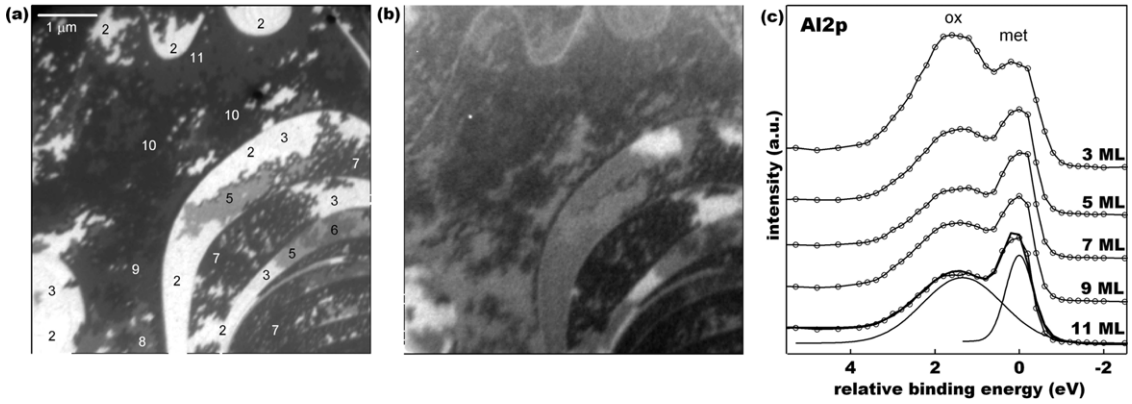

Figure 3. (a) LEEM image (3.2 eV) of a typical Al/W(110) film; contrast is due to quantum size effects. The atomic thickness is indicated for the different grey levels. (b) XPEEM image after exposure to 18 L O_2, acquired on the high binding energy 'ox' shoulder of the Al 2p core level. (c) The sample Al 2p core level spectra from different single-thickness areas, obtained by spectromicroscopy at the same oxygen exposure ($E_{\text{phot}} = 124$ eV). A typical fit using metallic ('met') and oxide-related ('ox') components is shown for the 11 ML spectrum.

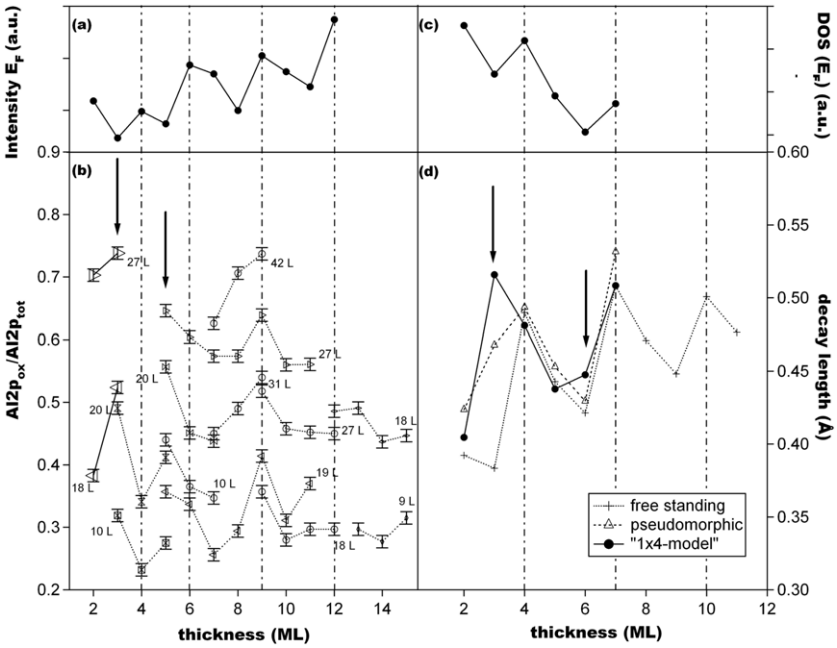

Figure 4. (a) Measured normal emission photoemission intensity of the Al films at E_F. (b) Summary of the oxidation efficiency as a function of thickness as obtained in different experimental runs using freshly prepared Al layers. Data with the same marker correspond to the same O_2 exposure. The error bars are realistic for comparison of data from the same batch (exposure). In contrast, only qualitative comparison can be made between different exposures, since the largest experimental error is in the exposure. (c) Calculated DOS per atom of the Al films at the Fermi level. (d) Calculated electronic density decay length. Dashed lines indicate the thickness at which a QWS crosses E_F. Arrows highlight the main changes in λ (see the text).

changing the strain conditions of the film, from unstrained to pseudomorphic, has virtually no effect on the QWS peak positions (figure 2(b)) and decay length maxima (figure 4(d)). This is related to the fact that, contrary to the case of the Mg films, the surface area per atom of the Al films remains essentially unchanged.

Figure 2(b) presents the calculated Al LDOS for the supported films in the pseudomorphic and '1 × 4-model' configuration and the energy levels at $\bar{\Gamma}$ for the free-standing film (here the Shockley surface and interface state are both labelled SS). In the high binding energy part of the spectrum, from 6 to 10 eV below E_F, the QWSs become broad resonances in the presence of W. Outside that region, however, only very small differences are observed in the peak positions between the three configurations (in particular, in the region from 6 eV below to 2 eV above E_F). Hence, the presence of the substrate, interface, and epitaxial strain, has no significant influence on the sequence of thicknesses at which the QWS peak maxima cross E_F. The very weak dependence we find for the peak positions on the strain conditions of the film is attributed to the fact that the surface area per atom of the film remains essentially unchanged in the three cases (less than 1% change in the surface area per atom between unstrained/relaxed and coherently strained Al films on W), in spite of the large individual changes in ε_{xx} and ε_{yy}.

The Al films were exposed up to ∼50 Langmuir (L) O_2 at room temperature. Under these conditions, oxidation is limited to the topmost atomic layers, concomitant with the high surface sensitivity of our XPEEM measurements (photoelectron escape depth ∼3 Å [36]). The variations of the initial oxidation rate with film thickness were quantitatively determined by measuring the intensity of the chemically shifted 'oxide' component (I_{ox}) in the Al 2p spectra, which is proportional to the number of Al atoms bound to O. Due to the moderate energy resolution in spectromicroscopy mode, a broad Gaussian was used for the I_{ox} component in order to account for the different oxygen–Al bonding configurations that were identified by high resolution spectroscopy [37–39]. Thus, the intensity of the I_{ox} feature, which can be reliably identified for oxygen coverage below 0.1 ML, is used as a measure of relative *total* oxygen intake of each surface region, without distinction between chemisorbed and true alumina phase (the former strongly dominating in the explored regime). Already visual inspection of the LEEM and XPEEM images in figures 3(a) and (b) and the Al 2p spectra taken from single-thickness regions in figure 3(c) reveal a clear thickness dependence of the oxidation rate; e.g. 3, 5, and 9 ML films oxidize faster. We stress that all experiments were carried out in the chemisorption regime, where most of the film remains metallic while islands of O-bonded Al form on the surface.

The measured normal emission photoelectron intensity at E_F, with maxima at 4, 6, 9, and 12 ML, when a new QWS becomes occupied, is shown in figure 4(a). The dependence of the Al oxidation rate on film thickness obtained from several sets of LEEM–XPEEM experiments is summarized in figure 4(b). Each data point is obtained by fitting a local Al 2p spectrum, and data from the same oxygen exposure have the same symbol. There are local maxima in the oxidation extent at 3 ML, 5 ML, 9 ML, and a weaker one at 12 ML at low-oxygen exposure. The simple correlation between reactivity and DOS

observed for Mg films does not explain the higher reactivity of the 3 and 5 ML Al films. Figure 4(c) illustrates how not only the LDOS around the $\bar{\Gamma}$ point, but also the calculated integrated DOS per Al atom shows maxima at E_F each time a QWS becomes occupied.

The higher reactivity of the 3 and 5 ML Al films, i.e. for thicknesses one ML less than the crossing of E_F by a QWS, turns out to be a consequence of the influence of the substrate on the Al film electronic properties. Real films are often far from the ideal model of an infinite potential well due to interaction with the support, but even if such effects have been recognized in experiments [40–44], the computational difficulties have prevented realistic modelling of non-pseudomorphic interfaces.

Our calculations for the pseudomorphic 3 ML Al film show that mixing of the first unoccupied QWS with W states results in a broadened resonance, centred above E_F, but with finite electronic population (figure 2). This QWS resonance, being nearer to the vacuum level at $\bar{\Gamma}$, has an increased decay length into vacuum. This increases λ calculated following [18], for 3 ML, as can be seen in figure 4(d), where we compare the calculated λ for the three model structures. Hybridization with the substrate states, and hence λ, is even larger for the '1×4-model' film. The decay length for 3 ML is a minimum in the free-standing film but a strong local maximum in the (1×4)-configuration, explaining why, despite having a low electron density, the 3 ML film has a higher reactivity than 2 and 4 ML films.

For the same reason, as the model becomes more realistic, the calculated λ increases with respect to the neighbour thicknesses also for 6 ML (both cases are highlighted by arrows in figure 4(d)), but in this case does not become a maximum even in the '1×4-model'. This thickness is again one layer before the entrance of a new QWS below E_F, and, due to the rigid shift between theory and experiment, corresponds to the measured 5 ML Al film. The calculations in this case explain the experimental results only qualitatively, in the sense that they show increasing decay length for increasing interaction with the substrate. A possible explanation for the calculated $\lambda_{6\ \mathrm{ML}}$ not becoming a local maximum is that we have not accounted for the additional hybridization channels present in the real system due to the incommensurate interface above the bilayer, which make the interaction with the substrate stronger.

The correlation of electronic decay length and reactivity suggests an important role of non-adiabatic contributions to the O_2 molecule–Al surface interactions, i.e. the surface regions where electronic tails stretch further into the vacuum provide more electronic tunnelling/overlap probability before the molecule reaches the classical turning point in front of the surface. However, our work does not permit us to draw conclusions about the effect of O_2 ionization [16, 19], spin [21, 22], molecular rotations [20], or other parameters previously invoked.

In summary, the combination of electron microscopy experiments and state-of-the-art calculations demonstrates the importance of the substrate in order to understand the subtleties of the surface electronic structure. This work also demonstrates that the oscillations in the surface reactivity observed in ultrathin films of sp metals cannot be explained by variations of the density of states. We suggest that the electronic density decay length is responsible for the observed oscillations and that it could play an important role in the molecule–surface interaction for a wide variety of systems.

Acknowledgments

We thank M Altarelli for stimulating discussions. Support from the Light Source Theory Network of the EU is gratefully acknowledged.

References

[1] Hoffman R 1988 *Rev. Mod. Phys.* **60** 601–28
[2] Hammer B and Norskov J K 1995 *Surf. Sci* **343** 211–20
[3] Cohen M H, Ganduglia-Pirovano M V and Kudrnovsky J 1994 *Phys. Rev. Lett.* **72** 3222–5
[4] Wilke S, Cohen M H and Scheffler M 1996 *Phys. Rev. Lett.* **77** 1560–3
[5] Moriarty P 2001 *Rep. Prog. Phys.* **64** 297–381
[6] Rosei F 2004 *J. Phys.: Condens. Matter* **16** S1373–436
[7] Lauritsen J V *et al* 2003 *Nanotechnology* **14** 385–9
[8] Bell A T 2003 *Science* **299** 1688–91
[9] Rodriguez J A and Goodman D W 1992 *Science* **257** 897–903
[10] Roudgar A and Groß A 2003 *Phys. Rev.* B **67** 033409
[11] Schlapka A, Lischka M, Gross A, Krasberger U and Jakob P 2003 *Phys. Rev. Lett.* **91** 016101
[12] Aballe L, Barinov A, Locatelli A, Heun S and Kiskinova M 2004 *Phys. Rev. Lett.* **93** 196103
[13] Danese A G, Curti F G and Bartynski R A 2004 *Phys. Rev.* B **70** 165420
[14] Ma X, Jiang P, Qi Y, Jia J, Yang Y, Duan W, Li W X, Bao X, Zhang S B and Xue Q K 2007 *Proc. Natl Acad. Sci.* **104** 9204–8
[15] Zhang Z, Zhang Y, Fu Q, Zhang H, Yao Y, Ma T, Tan D, Xue Q and Bao X 2008 *J. Chem. Phys.* **129** 014704
[16] Hellman A 2005 *Phys. Rev.* B **72** 201403(R)
[17] Binggeli N and Altarelli M 2006 *Phys. Rev. Lett.* **96** 036805
[18] Binggeli N and Altarelli M 2008 *Phys. Rev.* B **78** 035438
[19] Hellman A, Razaznejad B, Yourdshahyan Y, Ternow H, Zoriç I and Lundqvist B I 2003 *Surf. Sci.* **532–535** 126–31
[20] Binetti M, Weisse O, Hasselbrink E, Katz G, Kosloff R and Zeiri Y 2003 *Chem. Phys. Lett.* **373** 366–71
[21] Behler J, Delley B, Lorenz S, Reuter K and Scheffler M 2005 *Phys. Rev. Lett.* **94** 036104
[22] Carbogno C, Behler J, Gross A and Reuter K 2008 *Phys. Rev. Lett.* **101** 096104
[23] Honkala K and Laasonen K 2000 *Phys. Rev. Lett.* **84** 705
[24] Yourdshahyan Y, Razaznejad B and Lundqvist B I 2002 *Phys. Rev.* B **65** 075416
[25] Sasaki T and Ohno T 1999 *Phys. Rev.* B **60** 7824–7
[26] Osterlund L, Zoriç I and Kasemo B 1997 *Phys. Rev.* B **55** 15452–5
[27] Brune H, Wintterlin J, Behm R J and Ertl G 1992 *Phys. Rev. Lett.* **68** 624–7
[28] Mosch C, Koukounas C, Bacalis N, Metropoulos A, Gross A and Mavridis A 2008 *J. Phys. Chem.* C **112** 6924–32
[29] Da Silva J L F 2005 *Phys. Rev.* B **71** 195416
[30] Aballe L *et al* 2009 in preparation
[31] Baroni S, Dal Corso A, de Gironcoli S and Giannozzi P, Plane-wave self-consistent field code http://www.pwscf.org

[32] Perdew J P, Burke K and Ernzerhof M 1996 *Phys. Rev. Lett.* **77** 3865–8
[33] Speer N J, Tang S J, Miller T and Chiang T C 2006 *Science* **314** 804–6
[34] Aballe L, Rogero C, Gokhale S, Kulkarni S and Horn K 2001 *Surf. Sci.* **482–485** 488–94
[35] Bross H 2004 *Eur. Phys. J.* B **37** 405
[36] Center for X-Ray Optics and Advanced Light Source 2001 *X-Ray Data Booklet 2001* (California, CA: Lawrence Berkeley National Laboratory)
[37] McConville C F, Seymour D L, Woodruff D P and Bao S 1987 *Surf. Sci.* **188** 1–14
[38] Berg C, Raaen S, Borg A, Andersen J N, Lundgren E and Nyholm R 1993 *Phys. Rev.* B **47** 13063–6
[39] Driver S M *et al* 1997 *Surf. Sci.* **391** 300–14
[40] Mueller M A, Samsavar A, Miller T and Chiang T C 1989 *Phys. Rev.* B **40** 5845–8
[41] Aballe L, Rogero C, Kratzer P, Gokhale S and Horn K 2001 *Phys. Rev. Lett.* **87** 156801
[42] Upton M H, Miller T and Chiang T C 2005 *Phys. Rev.* B **71** 033403
[43] Moras P, Weisskopf Y, Longchamp J N, Erbudak M, Zhou P H, Ferrari L and Carbone C 2006 *Phys. Rev.* B **74** 121405(R)
[44] Wei C M and Chou M Y 2003 *Phys. Rev.* B **68** 125406